

# Evaluation of left ventricular function in patients with acute ischaemic stroke using cine cardiovascular magnetic resonance imaging

Simon Hellwig<sup>1,2\*</sup> , Ulrike Grittner<sup>3,7</sup>, Matthias Elgeti<sup>4</sup>, Sebastian Wyschkon<sup>5</sup>, Sebastian N. Nagel<sup>5</sup>, Jochen B. Fiebach<sup>2</sup>, Thomas Krause<sup>6</sup>, Juliane Herm<sup>1,2</sup>, Jan F. Scheitz<sup>1,2,7,9</sup>, Matthias Endres<sup>1,2,7,8,9</sup>, Christian H. Nolte<sup>1,2,7,8,9</sup>, Karl Georg Haeusler<sup>10</sup> and Thomas Elgeti<sup>5</sup>

<sup>1</sup>Department of Neurology, Charité—Universitätsmedizin Berlin, Berlin, Germany; <sup>2</sup>Centre for Stroke Research Berlin, Charité—Universitätsmedizin Berlin, Berlin, Germany;

<sup>3</sup>Institute of Biometry and Clinical Epidemiology, Charité—Universitätsmedizin Berlin, Berlin, Germany; <sup>4</sup>Jules Stein Eye Institute and Department for Chemistry and Biochemistry, University of California, Los Angeles, CA, USA; <sup>5</sup>Department of Radiology, Charité—Universitätsmedizin Berlin, Berlin, Germany; <sup>6</sup>Department of Neurology, Jüdisches Krankenhaus Berlin, Berlin, Germany; <sup>7</sup>Berlin Institute of Health, Berlin, Germany; <sup>8</sup>German Centre for Neurodegenerative Diseases (DZNE), partner site Berlin, Berlin, Germany; <sup>9</sup>German Centre for Cardiovascular Diseases (DZHK), partner site Berlin, Berlin, Germany; <sup>10</sup>Department of Neurology, Universitätsklinikum Würzburg, Würzburg, Germany

## Abstract

**Aims** Heart failure (HF) is frequent in patients with acute ischaemic stroke (AIS) and associated with higher morbidity and mortality. Assessment of cardiac function in AIS patients using cardiovascular MRI (CMR) may help to detect HF. We report the rate of systolic and diastolic dysfunction in a cohort of patients with AIS using CMR and compare cine real-time (CRT) sequences with the reference of segmented cine steady-state free precession sequences.

**Methods and results** Patients with AIS without known atrial fibrillation were prospectively enrolled in the HEart and BRain Interfaces in Acute Ischemic Stroke (HEBRAS) study (NCT 02142413) and underwent CMR at 3 Tesla within 7 days after AIS. Validity of CRT sequences was determined in 50 patients. A total of 229 patients were included in the analysis (mean age 66 years; 35% women; HF 2%). Evaluation of cardiac function was successful in 172 (75%) patients. Median time from stroke onset to CMR was 82 h (interquartile range 56–111) and 54 h (interquartile range 31–78) from cerebral MRI to CMR. Systolic dysfunction was observed in 43 (25%) and diastolic dysfunction in 102 (59%) patients. Diagnostic yield was similar using CRT or segmented cine imaging (no significant difference in left ventricular ejection fraction, myocardial mass, time to peak filling rate, and peak filling rate ratio E/A). Intraobserver and interobserver agreement was high ( $\kappa = 0.78\text{--}1.0$  for all modalities).

**Conclusions** Cardiovascular MRI at 3 Tesla is an appropriate method for the evaluation of cardiac function in a selected cohort of patients with AIS. Systolic and diastolic dysfunction is frequent in these patients. CRT imaging allows reliable assessment of systolic and diastolic function.

**Keywords** Heart failure; Cine real-time; Cardiac MRI; Diastolic dysfunction; Volume–time curve; Acute ischaemic stroke

Received: 24 February 2020; Revised: 5 May 2020; Accepted: 27 May 2020

\*Correspondence to: Simon Hellwig, MD, MSc, Department of Neurology, Charité—Universitätsmedizin Berlin, Campus Benjamin Franklin, Hindenburgdamm 30, 12203 Berlin, Germany. Tel: +49(30)450560697; Fax: +49(30)4507560965.

Email: simon.hellwig@charite.de

[Correction added on July 22, 2020, after first online publication: Projekt Deal funding statement has been added.]

## Introduction

About 9% of all ischaemic strokes are believed to originate from chronic heart failure (HF).<sup>2</sup> At the same time, HF is a common comorbidity with a prevalence of 10–24% among stroke patients.<sup>3</sup> While half of all patients with chronic HF present with reduced left ventricular ejection fraction

[LVEF < 50%, HF with reduced ejection fraction (HFrEF)], impaired diastolic properties but preserved ejection fraction (LVEF ≥ 50%, HF with preserved ejection fraction) are present in the other half. Current guidelines also differentiate LVEF in the range of 40–49% (HF with mid-range ejection fraction).<sup>4,5</sup> To date, HF with preserved ejection fraction is the most common manifestation of HF with a median prevalence of 4–7%

as compared with 2–6% for HFrEF in patients aged 60 years and older, using echocardiography.<sup>6</sup> Left ventricular diastolic dysfunction without manifest HF is even more frequent in these patients with a median prevalence of 16–53% in comparison with 3–9% for systolic dysfunction.<sup>6</sup> However, data regarding the prevalence of left ventricular diastolic dysfunction in patients with acute ischaemic stroke (AIS) are limited.<sup>7–9</sup> Few studies have investigated the role of cardiovascular MRI (CMR) in comparison with transthoracic echocardiography in the diagnostic workup after AIS, providing incongruent results.<sup>10–12</sup>

Cardiovascular MRI is a radiation-free, non-invasive technique that offers excellent tissue contrast and does not rely on an acoustic window.<sup>13</sup> It is a promising diagnostic alternative for the evaluation of cardiac function in patients with AIS.<sup>12,14</sup> To our knowledge, there are no data available on systolic and diastolic function assessed by CMR in patients with AIS. We used CMR at 3 Tesla for the evaluation of left ventricular function after AIS, analysing volume-time curves (VTCs) generated by delineation of endocardial contours and planimetry of the left atrium.

K-space segmented cine steady-state free precession (SSFP) is considered standard of reference for assessment of cardiac function by CMR.<sup>15,16</sup> However, k-space segmented imaging determines image information from multiple heartbeats and therefore requires sinus rhythm. Cine real-time (CRT) imaging collects all necessary image information out of one single heartbeat; therefore, breath-holding periods are shorter and trigger artefacts can be overcome. The aims of this study are (i) to report systolic and diastolic cardiac function in a cohort of patients with AIS using CMR and (ii) to compare accelerated CRT images to the reference of segmented cine SSFP sequences for the analysis of systolic and diastolic left ventricular function.

## Methods

### Study design

This is a post hoc analysis of CMR examinations performed in patients participating in the HEart and BRain Interfaces in Acute Ischemic Stroke (HEBRAS) study. Patients with AIS (proven by brain MRI or computed tomography) and without history of atrial fibrillation were eligible to participate and had to provide written informed consent within 6 days after stroke onset. A first ever diagnosis of atrial fibrillation during the course of the study did not represent a reason for study discontinuation. The study protocol is described in detail elsewhere.<sup>17</sup> The study was approved by the Ethics Committee of the Charité—Universitätsmedizin Berlin (EA1/045/14) and registered online (NCT02142413).

### Magnetic resonance imaging

Cardiovascular MRI was performed on a 3 Tesla magnetic resonance (MR) scanner (MAGNETOM® TIM TRIO, Siemens, Erlangen, Germany) using electrocardiogram and pulse triggering. CMR was performed on Day 1 after study inclusion *per protocol*. Localization and planning were based on a dark-blood-prepared half-Fourier acquisition single-shot turbo spin echo sequence with the following parameters: repetition time (TR), 750 ms; echo time (TE), 49 ms; flip angle, 160°; slice thickness, 5 mm; and field of view/matrix. Left ventricular cardiac function was assessed in double-oblique cine SSFP technique. In accordance with current recommendations, two-chamber, three-chamber, and four-chamber views were acquired.<sup>18</sup> Short-axis examinations of the left ventricle were obtained parallel to the atrioventricular plane with prior individual frequency adjustment [TR 40.32 ms, TE 1.48 ms, flip angle 50°, matrix size 256 × 216 pixel, slice thickness 8 mm (2 mm interslice gap)].<sup>18</sup> Integrated parallel imaging techniques with twofold acceleration were used for short-axis stack acquisition. Following standard k-space segmented SSFP imaging, a fast SSFP real-time sequence (CRT) was used for short-axis cine imaging [TR 48.6 ms, TE 1.21 ms, flip angle 55°, matrix size 128 × 54 pixel, slice thickness 8 mm (2 mm interslice gap)] with threefold acceleration (integrated parallel imaging technique). ECG triggering was performed every second heartbeat to capture the entire diastole.

### Statistical analysis

The results are reported as absolute and relative frequencies for categorical variables. In the case of continuous variables, mean and standard deviation are reported for sufficiently normally distributed data ( $|\text{skewness}| < 1$ ) or median and limits of interquartile range (IQR) for variables with skewed distribution or ordinal variables. The Student's *t*-test for paired samples with continuous variables was used to compare parameters of left ventricular function in those patients who received both standard cine SSFP and CRT sequences. For all comparisons, cine SSFP imaging served as the accepted gold standard.<sup>15,16</sup> In accordance with the recommendations of Bland and Altman, differences of the parameters were plotted against the mean between the two methods.<sup>19</sup> Intraclass correlation coefficient (ICC) was calculated to account for intraobserver and interobserver variability. Additionally, Cohen's kappa was calculated for ordinal variables. McNemar's test was used for the comparison of paired samples with dichotomized variables. Furthermore, we calculated sensitivity, specificity, as well as positive and negative predictive values with regard to the defined gold standard of segmented cine SSFP sequences. In the case of categorical variables and independent samples, Pearson's  $\chi^2$  test was

used, whereas the Mann–Whitney  $U$  test was implemented as a rank sum test for ordinal variables. A two-sided significance level of  $\alpha = 0.05$  was considered. No adjustment for multiple testing was applied in this exploratory study. To account for the reproducibility of results, we calculated intraobserver and interobserver variability. Data were analysed using SPSS statistics 23 (IBM Corp., Armonk, NY, USA).

## Quantitative analysis of volume–time curves

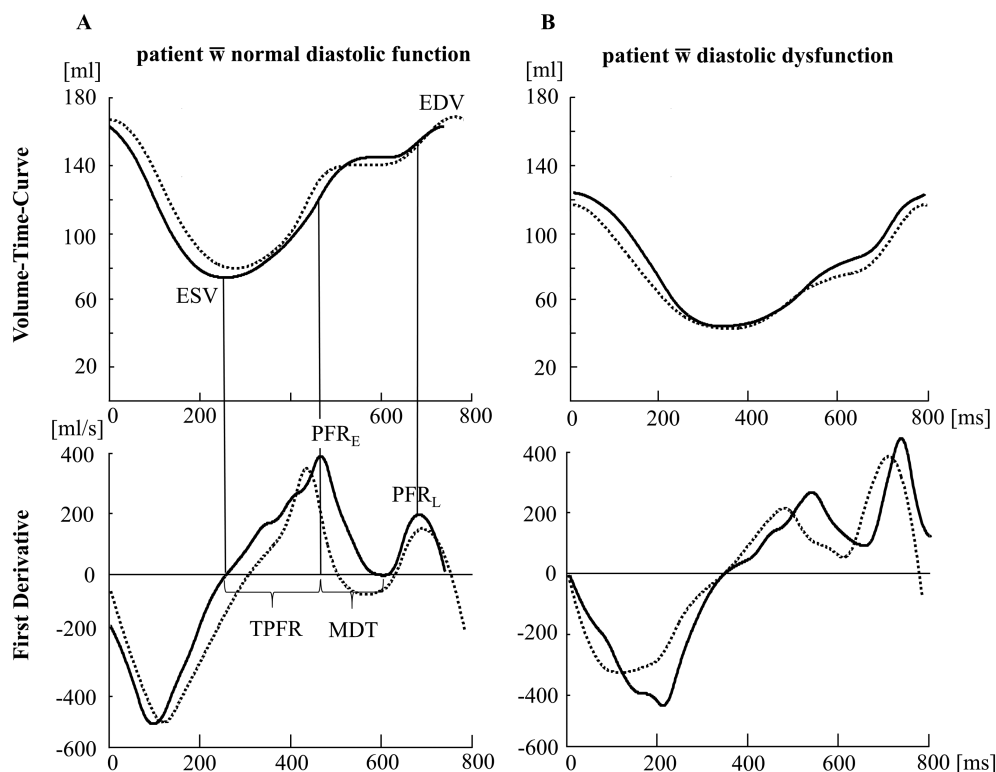
A physician (SH) trained and supervised by a radiologist with more than 10 years of experience in CMR (TE) evaluated all cases. By delineating endocardial contours of the left ventricle in each short-axis stack, individual VTCs were generated using cvi42®software (Circle Cardiovascular Imaging Inc., Calgary, Canada). Papillary muscles were allocated to the left ventricular cave.<sup>20</sup> Additionally, epicardial contours were delineated in systolic and diastolic phase to calculate left ventricular myocardial mass. VTCs and their first derivative were subsequently analysed using a semi-automated script in MATLAB® (MathWorks, Natick, Massachusetts, USA, version R2009a) in accordance with prior publications.<sup>21</sup> A spline algorithm was implemented to generate a smoothed VTC

with a time interval of 1 ms.<sup>22</sup> All curves were normalized to the maximal end-diastolic volume (EDV) at  $t = 0$ . Figure 1 shows VTC and first derivative from segmented as well as CRT sequences of a patient with normal diastolic function as well as of a patient with grade 1 diastolic dysfunction. The following parameters were calculated: EDV, end-systolic volume (ESV, zero crossing of the first derivative), peak filling rate early (PFR<sub>E</sub>, first maximum of the first derivative), peak filling rate late (PFR<sub>L</sub>, second maximum of the first derivative), time to peak filling rate early (TPFR), and mitral deceleration time (MDT).<sup>23</sup> The filling rate ratio E/A was calculated by dividing PFR<sub>E</sub> (E) by PFR<sub>L</sub> (A). Systolic dysfunction was defined as LVEF < 50%.<sup>5</sup> Diastolic dysfunction was graded as 0 (normal function), 1 (impaired relaxation), 2 (pseudonormal), or 3 (restrictive) using VTC-derived E/A ratio and left atrial planar size according to published recommendations.<sup>24</sup> For further statistical analysis, we dichotomized diastolic cardiac function into the categories ‘healthy’ and ‘abnormal’.

## Intraobserver and interobserver variability

A senior radiologist with experience in CMR (TE) evaluated endocardial and epicardial contours and subsequent VTCs

**FIGURE 1** Volume–time curves and their first derivative representing the cardiac cycle of a patient with normal diastolic function (A) and of a patient with diastolic dysfunction grade 1 (B) (modified from Hellwig<sup>1</sup>). The black line represents data derived from segmented cine SSFP images; the dotted line represents data derived from evaluation of cine real-time images. The assessment of diastolic parameters PFR<sub>E</sub>, PFR<sub>L</sub>, TPFR, and MDT is exemplified in (A). A small difference in the length of the cardiac cycle due to varying heart rate in (A) can be noted.



for 10 randomly chosen data sets of standard cine and CRT images, blinded for clinical and diagnostic information. Additionally, the first rater reevaluated the same 10 patients 6 months after the first reading. Measures of agreement were calculated for individual parameters of cardiac function as well as for the categorical classification of diastolic dysfunction.

## Results

In total, 2473 stroke patients were screened for participation in the HEart and BRain Interfaces in Acute Ischemic Stroke study between 1 May 2014 and 31 December 2015. With regard to inclusion and exclusion criteria, 374 patients were

eligible for participation, of which 230 patients provided written informed consent. One patient was excluded from the analysis because of non-ischaemic origin of symptoms (epileptic seizure), leaving 229 patients for analysis. *Table 1* shows the baseline characteristics of these patients. In total, 185 patients (81%) underwent CMR, with completed short-axis cine imaging in 172 cases (75%). Standard cine SSFP imaging was performed in 166 patients (73%), and 56 patients (25%) received additional CRT imaging. Both modalities were acquired in 50 participants (22%).<sup>1</sup> Median examination time for the complete CMR protocol (including contrast-enhanced sequences, i.e. MR angiography and late enhancement imaging) was 41 min (IQR 35–48). Median examination time for short-axis cine SSFP imaging was 3:41 min (IQR 3:06–4:14), whereas CRT imaging was significantly shorter [median examination time 0:22 min (IQR 0:15–0:25,  $P = 0.005$ )]. An overview of the study profile is shown in *Figure 2*.

**Table 1** Baseline characteristics of 229 patients with acute ischaemic stroke and 50 patients that entered comparison of segmented cine SSFP and CRT sequences (modified from Hellwig<sup>1</sup>)

	All patients (N = 229)	SSFP vs. CRT (N = 50)
Female sex; n (%)	79 (34.5)	16 (32.0)
Age in years; mean (SD)	66 (12)	65 (13)
Length of in-hospital stay (days); median (IQR)	6 (5–7)	5 (5–6)
Cerebral CT; n (%)	139 (60.7)	21 (42.0)
Without contrast agent	125 (54.6)	20 (4.0)
Including angiography	14 (6.1%)	1 (2.0%)
Cerebral MRI; n (%)	226 (98.7)	50 (100)
Cardiac MRI; n (%)	185 (80.8)	50 (100)
NIHSS on admission; median (IQR)	2 (1–4)	2 (1–4)
NIHSS at discharge; median (IQR)	0 (0–2)	0 (0–1)
mRS on admission; median (IQR)	2 (1–3)	2 (1–2)
mRS at discharge; median (IQR)	1 (0–2)	1 (0–1)
Barthel index on admission; median (IQR)	100 (80–100)	100 (80–100)
Barthel index at discharge; median (IQR)	100 (95–100)	100 (100–100)
Intravenous thrombolysis; n (%)	46 (20.1)	7 (14.0)
Diabetes mellitus; n (%)	55 (24.0)	12 (24.0)
Arterial hypertension; n (%)	162 (70.7)	32 (64.0)
Chronic heart failure; n (%)	5 (2.2)	2 (4.0)
High blood lipids; n (%)	121 (52.8)	31 (62.0)
Previous ischemic stroke or TIA; n (%)	54 (23.6)	10 (20.0)
Current tobacco use; n (%)	70 (30.6)	16 (32.0)
Acetylsalicylic acid; n (%)	66 (28.8)	11 (22.0)
Clopidogrel; n (%)	6 (2.6)	1 (2.0)
Dual antiplatelet therapy; n (%)	5 (2.2)	1 (2.0)
Oral anticoagulation; n (%)	3 (1.3)	
Phenprocoumon	1 (0.4)	
Rivaroxaban (20 mg)	2 (0.9)	
Beta-blockers; n (%)	71 (31.0)	16 (32.0)
ACE inhibitors; n (%)	45 (19.7)	7 (14.0)
Angiotensin II receptor antagonists; n (%)	46 (20.1)	15 (30.0)
Calcium channel blockers; n (%)	39 (17.0)	8 (16.0)
Statins; n (%)	59 (25.8)	9 (18.0)

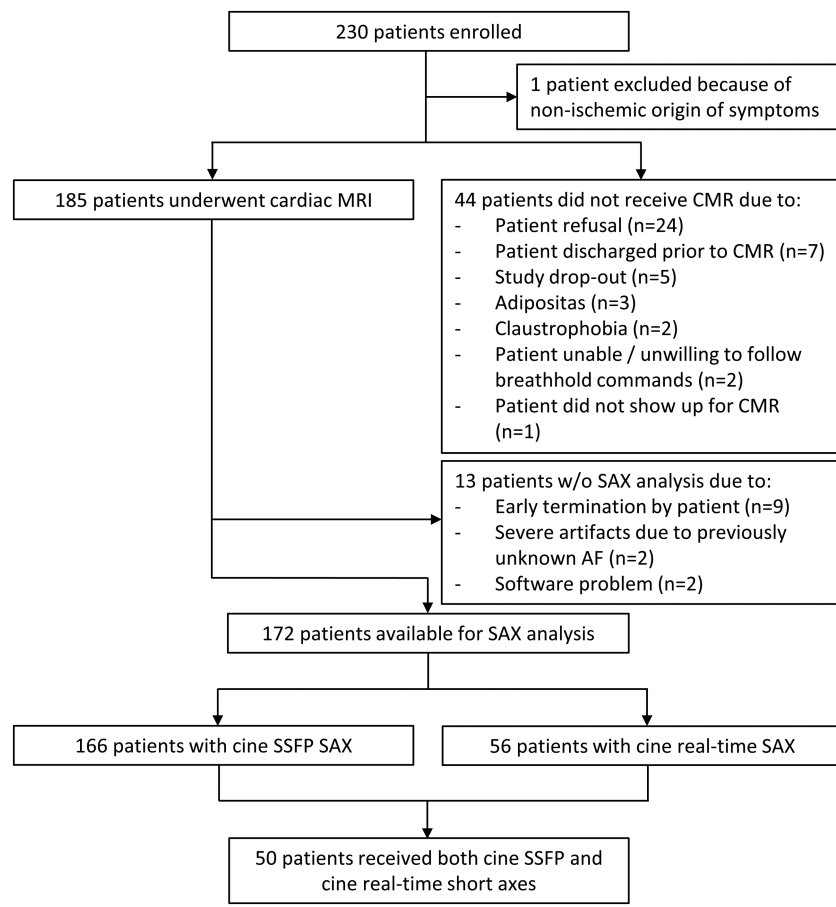
ACE, angiotensin-converting enzyme; CRT, cine real time; CT, computed tomography; IQR, interquartile range; MRI, magnetic resonance imaging; mRS, Modified Rankin Scale; NIHSS, National Institutes of Health Stroke Scale; SD, standard deviation; SSFP, steady-state free precession; TIA, transient ischaemic attack.

## Functional analysis and comparison of imaging modalities

Taken together, 43 out of 172 patients (25%) were found to have a reduced LVEF < 50%. VTC analysis revealed abnormal diastolic function in 102 of 172 patients (59%). Grade 1 diastolic dysfunction was found in 62 patients (36%), Grade 2 in 16 patients (9%), and Grade 3 in 24 patients (14%). Isolated systolic dysfunction was observed in 13 (8%), isolated diastolic dysfunction in 72 (42%), and a combination of both in 30 (17%) patients.<sup>1</sup>

## Comparison of segmented cine steady-state free precession and cine real-time imaging

We compared results from segmented cine SSFP and CRT imaging in 50 patients. Key parameters of cardiac function as derived from both modalities are shown in *Table 2*. Almost no or only slight differences were found for LVEF [mean difference: 0, 95% confidence interval (CI): −2 to 2], end-diastolic myocardial mass (EDMM) (mean difference: 4, 95% CI: −2 to 10), TPFR (mean difference: −3, 95% CI: −15 to 10) and E/A ratio (mean difference: −0.08, 95% CI: −0.25 to 0.1). EDV (mean difference: 6, 95% CI: 2 to 10), ESV (mean difference: 4, 95% CI: 1 to 7), PFR<sub>E</sub> (mean difference 32, 95% CI: 12 to 51), PFR<sub>L</sub> (mean difference: 38, 95% CI: 9 to 67), and MDT (mean difference: −7, 95% CI: −11 to −3) showed statistically significant differences between both groups. Corresponding diagrams according to the method of Bland and Altman can be found in the Supporting Information. Bland–Altman plots demonstrate underestimation of EDV, ESV, PFR<sub>E</sub>, and PFR<sub>L</sub> values and overestimation of MDT values over the whole range of values.

**FIGURE 2** Overview of the study profile. SAX, short axis; AF, atrial fibrillation.

These 50 patients were also categorized as ‘healthy’ (systolic function: LVEF  $\geq$  50%, diastolic function: no sign of

**Table 2** Comparison of segmented cine SSFP and cine real-time imaging

	Segmented cine SSFP Mean (SD)	Cine real-time Mean (SD)	Mean difference (95% CI)
EDV	141 (53)	135 (50)	6 (2 to 10)
ESV	70 (49)	66 (47)	4 (1 to 7)
LVEF	53 (13)	53 (14)	0 (-2 to 2)
EDMM	102 (39)	99 (36)	4 (-2 to 10)
PFR <sub>E</sub>	318 (112)	286 (114)	32 (12 to 51)
TPFR	155 (40)	158 (37)	-3 (-15 to 10)
PFR <sub>L</sub>	304 (100)	266 (105)	38 (9 to 67)
E/A	1.15 (0.56)	1.23 (0.66)	-0.08 (-0.25 to 0.10)
MDT	55 (15)	62 (14)	-7 (-11 to -3)

E/A, peak filling rate ratio; EDMM, end-diastolic myocardial mass (g); EDV, end-diastolic volume (mL); ESV, end-systolic volume (mL); LVEF, left ventricular ejection fraction (%); MDT, mitral deceleration time (ms); PFR<sub>E</sub>, peak filling rate early (mL/min); PFR<sub>L</sub>, peak filling rate late (mL/min); SSFP, steady-state free precession; TPFR, time to peak filling rate (ms).

Segmented cine SSFP and cine real-time sequences were acquired in 50 patients and analysed for the determination of key parameters of cardiac function (modified from Hellwig<sup>1</sup>).

diastolic dysfunction) or ‘abnormal’ (systolic function: LVEF  $<$  50%, diastolic function: any sign of diastolic dysfunction). With regard to systolic function, 42 of 50 patients (84%) and with regard to diastolic function, 35 of 50 patients (70%) were equally categorized according to both modalities. The proportion of patients with unequal categorization was similar in both modalities (systolic function: 6% vs. 10%, diastolic function: 12% vs. 18%; McNemar’s test for marginal homogeneity: systolic function  $P = 0.61$ ; diastolic function  $P = 0.73$ ). Measures of classification accuracy were as follows: for systolic cardiac function, sensitivity of CRT was 85.7% and specificity 80.0%. For diastolic cardiac function, sensitivity of CRT was 74.3% and specificity was 60.0%. The positive and negative predictive value of CRT for systolic cardiac function was 91.0% and 71.0% and 81.0% and 50.0% for diastolic cardiac function, respectively.<sup>1</sup>

### Intraobserver and interobserver variability

Supporting Information, *Tables S1* and *S2* display the results from intraobserver and interobserver comparison for

individual parameters of cardiac function from 10 randomly chosen data sets. ICCs for parameters directly derived from the delineation of imaging data (EDV, ESV, LVEF, and EDMM) were all above 0.83. There was a comparatively low level of agreement (ICC below 0.5) for selected variables deduced from the first derivative of imaging data: for intraobserver comparison from CRT data regarding TPFR (0.44) and MDT (0.36) as well as for the interobserver comparison from segmented cine SSFP data regarding PFR<sub>E</sub> (0.35), E/A ratio (0.16), and MDT (0.25) and from CRT data PFR<sub>E</sub> (−0.15), PFR<sub>L</sub> (0.35), E/A ratio (−0.2), and MDT (0.34). Cohen's kappa for dichotomous intraobserver and interobserver grading ('healthy' vs. 'abnormal') of systolic function did not differ for cine SSFP and CRT imaging ( $\kappa = 1.0$ ). Intraobserver grading of diastolic function differed in one case for CRT analysis ( $\kappa = 0.78$ ) and was consistent for standard cine analysis ( $\kappa = 1.0$ ). Regarding interobserver comparison, grading of diastolic function differed in one case for standard cine imaging ( $\kappa = 0.78$ ) and did not disagree for CRT analysis ( $\kappa = 1.0$ ).

## Discussion

Assessment of systolic and diastolic cardiac function in patients with AIS using CMR at 3 Tesla was technically successful in the majority of included patients (75%). The rate of systolic dysfunction as assessed by CMR (25%) appears to be slightly above previous findings, which state a rate of HFrEF in ischaemic stroke patients of 10–24% using echocardiography.<sup>3</sup> However, one has to bear in mind that a borderline reduced LVEF does not necessarily result in clinically manifest HF. A recent systematic review reports a rate of diastolic dysfunction between 16–53% in a population of patients aged 60 and older, based on echocardiographic findings.<sup>6</sup> In our analysis, diastolic dysfunction was present in 59% of patients, using CMR criteria. Because only five patients (2%) had a medical history of HF, CMR supposedly also detects minor, supposedly asymptomatic impairment of diastolic function.

In comparing accelerated CRT sequences with standard high-resolution cine SSFP images, we found sufficient agreement for the evaluation of systolic and diastolic cardiac function with regard to key parameters such as TPFR and the peak filling rate ratio E/A. Sensitivity and specificity of CRT analysis were good for the assessment of systolic and sufficient for the assessment of diastolic function. Our findings are of high clinical importance, because reduced examination time is crucial for the evaluation of potentially severely impaired patients suffering from AIS.<sup>12</sup> Atrial fibrillation is frequent among patients with ischaemic stroke, and possible avoidance of triggering artefacts due to irregular heartbeat may represent another advantage in favour of CRT imaging. However, because we did not include patients with known atrial fibrillation, we are unable to prove this assumption. Furthermore, we observed no

statistically significant difference between the two modalities with respect to LVEF and EDMM, whereas ESV and EDV did differ significantly. However, given the small absolute magnitude of the mean difference (4 and 6 mL, respectively), we do not believe that this is of clinical importance.

Comparison of standard cine SSFP and CRT imaging at 3 Tesla revealed similar differences as previously described for 1.5 Tesla.<sup>25</sup> Similar to studies comparing segmented cine SSFP and segmented cine gradient recall echo sequences, our study revealed differences in ESV and EDV, supposedly due to better delineation of the endocardial contour.<sup>26</sup> Therefore, the need for specific normal values depending on the spatial and temporal resolution used in CRT sequences is necessary. The aforementioned statistically significant differences between parameters ESV, EDV, PFR<sub>E</sub>, PFR<sub>L</sub>, and MDT despite only small variances regarding the respective mean values and standard deviations might partly be explainable by systematically increased individual values in the analysis of high-resolution standard cine SSFP images due to a more precise delineation of the endocardial contour and the improved temporal resolution for volumes, whereas the differences of temporal rates and times might be amplified due to the use of the derivative.<sup>27</sup> In the future, new imaging reconstruction techniques such as regularized non-linear inversion might enhance assessment of cardiac function.<sup>28</sup>

Intraobserver and interobserver variability was negligible for key parameters of cardiac function (EDV, ESV, LVEF, and EDMM), which underlines the reputation of CMR as a robust and reproducible method.<sup>29</sup> A comparatively low level of agreement (ICC below 0.5) for selected variables deduced from the first derivative of the VTC (PFR<sub>E</sub>, TPFR, PFR<sub>L</sub>, E/A ratio, and MDT) may result from small deviations due to different temporal resolution (cine SSFP: TR 40.3 ms, CRT: TR 48.6 ms) that can be amplified by the derivative.<sup>27</sup>

By demonstrating that CMR at 3 Tesla is an appropriate method for the evaluation of cardiac function in a selected cohort of patients with AIS, we believe that this represents a useful complement in the diagnostic workup after ischaemic stroke. However, we are aware that CMR requires certain physical and technical preconditions. In particular, severely impaired stroke patients might not be able to complete a full CMR examination or to comply with breath-holding commands. In our setting, CRT technique for short-axis acquisition was significantly shorter than cine SSFP imaging. Implementation of CRT imaging might thus help to reduce examination time. This may have practical implications, as a shorter total examination time may increase clinical feasibility.

## Limitations

This study has several limitations that might mitigate the validity of its results. First, this represents a post hoc analysis of a selected group of patients with AIS willing to undergo CMR. Our

findings cannot be generalized to all patients with AIS, as patients with atrial fibrillation or patients unable to provide informed consent were excluded.<sup>17</sup> Second, we only used MR-derived parameters for classification of cardiac function. With respect to the clinical gold standard of echocardiography, comparison of parameters of cardiac function would have been desirable. The threshold for normal systolic function was set to LVEF  $\geq 50\%$ , although one might argue that there is a scope of uncertainty between 35–50%, which was not specifically addressed.<sup>5</sup> Recently updated guidelines for the diagnosis and treatment of HF suggest a state of HF with mid-range ejection fraction (LVEF 40–49%).<sup>5</sup> However, we did not address this concept in our study, because it has not been introduced into clinical practice and was not available at the time of data analysis. Third, temporal resolution of real-time imaging was lower than for the segmented cine imaging, which biases particularly the functional assessment at higher heart rates and in diastole. Fourth, in accordance with reference literature, we used the left atrial planar size as a parameter to differentiate between normal and pseudonormal diastolic function.<sup>30</sup> Although prognostically relevant, some other factors that have been described to influence left atrial size such as adipositas or low blood haemoglobin were not adjusted for in our analysis.<sup>31,32</sup>

## Summary

Knowledge about the assessment of cardiac function using CMR at 3 Tesla in patients suffering from AIS is limited. Comparing standard segmented cine SSFP sequences and accelerated CRT sequences, the latter showed a sufficient level of agreement for the determination of key functional parameters but requires determination of specific normal values with regard to spatial and temporal resolution. Whether contrast-enhanced CMR is of incremental diagnostic and prognostic value in the workup after AIS, especially in patients with previously unknown coronary artery disease, requires further investigation.

## Disclosure

This manuscript is based in part on data collected for the doctoral thesis of the first author.<sup>1</sup>

## Article Funding

Open access funding enabled and organized by Projekt DEAL.

## Conflict of interest

S.H., U.G., M.E., S.W., S.N., T.K., J.H., J.F.S., and T.E. report no conflicts of interest. J.B.F. was funded by the German Federal Ministry of Education and Research (01EO0801 and 01EO01301) and by the Berlin Institute of Health. J.B.F. has received consulting and advisory board fees from BioClinica, Cerevast, Artemida, Brainomix, Biogen, BMS, EISAI, and Guerbet. M.E. reports grants from Bayer and fees paid to the Charité from Bayer, Boehringer Ingelheim, BMS/Pfizer, Daiichi Sankyo, Amgen, GlaxoSmithKline GSK, Sanofi, Covidien, and Novartis, all outside the submitted work. C.H. N. reports lecture fees/advisory board fees from Boehringer Ingelheim, Pfizer, Bristol-Myers-Squibb, WL Gore & Associates, Abbott, as well as research grants by the Deutsches Zentrum für Herz-Kreislauftforschung (DZHK) und Deutsches Zentrum für neurodegenerative Erkrankungen (DZNE). K.G.H reports lecture fees and study grants by Bayer Healthcare, a study grant by Sanofi-Aventis, as well as lecture fees/advisory board fees from Bayer, Sanofi-Aventis, Boehringer Ingelheim, Daiichi Sankyo, Pfizer, Bristol-Myers-Squibb, Edwards Lifesciences, Medtronic, Biotronic, and WL Gore & Associates.

## Funding

This work was supported by the grant from Centre for Stroke Research Berlin (grant 01 EO 0801) from the German Federal Ministry of Education and Research.

## Supporting information

Additional supporting information may be found online in the Supporting Information section at the end of the article.

**Table S1.** Intraobserver variability. A) Segmented cine SSFP and B) cine real-time datasets from ten randomly chosen patients were reevaluated in a blinded fashion by the original rater to determine intraobserver variability (modified from<sup>1</sup>).

**Table S2.** Interobserver variability. A) Segmented cine SSFP and B) cine real-time datasets from ten randomly chosen patients were reevaluated in a blinded fashion by a second experienced rater to determine interobserver variability (modified from<sup>1</sup>).

## References

1. Hellwig S. *Kardiale 3 Tesla Magnetresonanztomographie zur Beurteilung der Herzfunktion bei Patienten mit akutem ischämischen Schlaganfall.* Klinik und Hochschulambulanz für Radiologie. Berlin: Charité - Universitätsmedizin Berlin; 2017 Available from: <https://doi.org/10.17169/refubium-16953>
2. Pullicino P, Homma S. Stroke in heart failure: atrial fibrillation revisited? *J Stroke Cerebrovasc Dis* 2010; **19**: 1–2.
3. Häusler KG, Laufs U, Endres M. Chronic heart failure and ischemic stroke. *Stroke* 2011; **42**: 2977–2982.
4. Dinatolo E, Sciatti E, Anker MS, Lombardi C, Dasseni N, Metra M. Updates in heart failure: what last year brought to us. *ESC Heart Fail* 2018; **5**: 989–1007.
5. Ponikowski P, Voors AA, Anker SD, Bueno H, Cleland JG, Coats AJ, Falk V, Gonzalez-Juanatey JR, Harjola VP, Jankowska EA, Jessup M, Linde C, Nihoyannopoulos P, Parissis JT, Pieske B, Riley JP, Rosano GM, Ruilope LM, Ruschitzka F, Rutten FH, van der Meer P, Authors/Task Force M. 2016 ESC Guidelines for the diagnosis and treatment of acute and chronic heart failure: the Task Force for the diagnosis and treatment of acute and chronic heart failure of the European Society of Cardiology (ESC) Developed with the special contribution of the Heart Failure Association (HFA) of the ESC. *Eur Heart J* 2016; **37**: 2129–2200.
6. van Riet EE, Hoes AW, Wagenaar KP, Limburg A, Landman MA, Rutten FH. Epidemiology of heart failure: the prevalence of heart failure and ventricular dysfunction in older adults over time. A systematic review. *Eur J Heart Fail* 2016; **18**: 242–252.
7. Seo JY, Lee KB, Lee JG, Kim JS, Roh H, Ahn MY, Park BW, Hyon MS. Implication of left ventricular diastolic dysfunction in cryptogenic ischemic stroke. *Stroke* 2014; **45**: 2757–2761.
8. Park HK, Kim BJ, Yoon CH, Yang MH, Han MK, Bae HJ. Left ventricular diastolic dysfunction in ischemic stroke: functional and vascular outcomes. *J Stroke* 2016; **18**: 195–202.
9. Ryu WS, Park JB, Ko SB, Hwang SS, Kim YJ, Kim DE, Lee SH, Yoon BW. Diastolic dysfunction and outcome in acute ischemic stroke. *Cerebrovasc Dis* 2016; **41**: 148–155.
10. Zahuranec DB, Mueller GC, Bach DS, Stojanovska J, Brown DL, Lisabeth LD, Patel S, Hughes RM, Attili AK, Armstrong WF, Morgenstern LB. Pilot study of cardiac magnetic resonance imaging for detection of embolic source after ischemic stroke. *J Stroke Cerebrovasc Dis* 2012; **21**: 794–800.
11. Baher A, Mowla A, Kodali S, Polsani VR, Nabi F, Nagueh SF, Volpi JJ, Shah DJ. Cardiac MRI improves identification of etiology of acute ischemic stroke. *Cerebrovasc Dis* 2014; **37**: 277–284.
12. Haeusler KG, Wollboldt C, Bentheim LZ, Herm J, Jager S, Kunze C, Eberle HC, Deluigi CC, Bruder O, Malsch C, Heuschmann PU, Endres M, Audebert HJ, Morguet AJ, Jensen C, Fiebach JB. Feasibility and diagnostic value of cardiovascular magnetic resonance imaging after acute ischemic stroke of undetermined origin. *Stroke* 2017; **48**: 1241–1247.
13. Adams L, Noutsias M, Bigalke B, Makowski MR. Magnetic resonance imaging in heart failure, including coronary imaging: numbers, facts, and challenges. *ESC Heart Fail*. 2018; **5**: 3–8.
14. Pagan RJ, Parikh PP, Mergo PJ, Gerber TC, Mankad R, Freeman WD, Shapiro BP. Emerging role of cardiovascular CT and MRI in the evaluation of stroke. *AJR Am J Roentgenol* 2015; **204**: 269–280.
15. Kramer CM, Barkhausen J, Flamm SD, Kim RJ, Nagel E. Society for Cardiovascular Magnetic Resonance Board of Trustees Task Force on Standardized P. Standardized cardiovascular magnetic resonance (CMR) protocols 2013 update. *J Cardiovasc Magn Reson* 2013; **15**: 91.
16. Puntmann VO, Valbuena S, Hinojar R, Petersen SE, Greenwood JP, Kramer CM, Kwong RY, McCann GP, Berry C, Nagel E, Group SCTW. Society for Cardiovascular Magnetic Resonance (SCMR) expert consensus for CMR imaging endpoints in clinical research: part I—analytical validation and clinical qualification. *J Cardiovasc Magn Reson* 2018; **20**: 67.
17. Haeusler KG, Grittner U, Fiebach JB, Endres M, Krause T, Nolte CH. HEart and BRain interfaces in Acute ischemic Stroke (HEBRAS)—rationale and design of a prospective observational cohort study. *BMC Neurol* 2015; **15**: 213.
18. Schulz-Menger J, Bluemke DA, Bremerich J, Flamm SD, Fogel MA, Friedrich MG, Kim RJ, von Knobelsdorff-Brenkenhoff F, Kramer CM, Pennell DJ, Plein S, Nagel E. Standardized image interpretation and post processing in cardiovascular magnetic resonance: Society for Cardiovascular Magnetic Resonance (SCMR) board of trustees task force on standardized post processing. *J Cardiovasc Magn Reson* 2013; **15**: 35.
19. Bland JM, Altman DG. Statistical methods for assessing agreement between two methods of clinical measurement. *Lancet* 1986; **1**: 307–310.
20. Duarte R, Fernandez-Perez G, Bettencourt N, Sampaio F, Miranda D, Franca M, Portugal P. Assessment of left ventricular diastolic function with cardiovascular MRI: what radiologists should know. *Diagn Interv Radiol* 2012; **18**: 446–453.
21. Zeidan Z, Erbel R, Barkhausen J, Hunold P, Bartel T, Buck T. Analysis of global systolic and diastolic left ventricular performance using volume-time curves by real-time three-dimensional echocardiography. *J Am Soc Echocardiogr* 2003; **16**: 29–37.
22. Schaafs LA, Wyschkon S, Elgeti M, Nagel SN, Knebel F, Steffen IG, Makowski MR, Hamm B, Elgeti T. Diagnosis of Left Ventricular Diastolic Dysfunction Using Cardiac Magnetic Resonance Imaging: Comparison of Volume-Time Curves Derived from Long- and Short-Axis Cine Steady-State Free Precession Datasets. *RoFo*. 2020. <https://doi.org/10.1055/a-1108-1892>
23. Bollache E, Redheuil A, Clement-Guinaudeau S, Defrance C, Perdriz L, Ladouceur M, Lefort M, De Cesare A, Herment A, Diebold B, Mousseaux E, Kachenoura N. Automated left ventricular diastolic function evaluation from phase-contrast cardiovascular magnetic resonance and comparison with Doppler echocardiography. *J Cardiovasc Magn Reson* 2010; **12**: 63.
24. Caudron J, Fares J, Bauer F, Dacher JN. Evaluation of left ventricular diastolic function with cardiac MR imaging. *Radiographics* 2011; **31**: 239–259.
25. Kunz RP, Oellig F, Krummenauer F, Oberholzer K, Romaneehsen B, Vomweg TW, Horstick G, Hayes C, Thelen M, Kreitner KF. Assessment of left ventricular function by breath-hold cine MR imaging: comparison of different steady-state free precession sequences. *J Magn Reson Imaging* 2005; **21**: 140–148.
26. Alfakih K, Plein S, Thiele H, Jones T, Ridgway JP, Sivananthan MU. Normal human left and right ventricular dimensions for MRI as assessed by turbo gradient echo and steady-state free precession imaging sequences. *J Magn Reson Imaging* 2003; **17**: 323–329.
27. Mendoza DD, Codella NC, Wang Y, Prince MR, Sethi S, Manoushagian SJ, Kawaiji K, Min JK, LaBounty TM, Devereux RB, Weinsaft JW. Impact of diastolic dysfunction severity on global left ventricular volumetric filling—assessment by automated segmentation of routine cine cardiovascular magnetic resonance. *J Cardiovasc Magn Reson* 2010; **12**: 46.
28. Frahm J, Voit D, Uecker M. Real-time magnetic resonance imaging: radial gradient-echo sequences with nonlinear inverse reconstruction. *Invest Radiol* 2019; **54**: 757–766.
29. Mooij CF, de Wit CJ, Graham DA, Powell AJ, Geva T. Reproducibility of MRI

- measurements of right ventricular size and function in patients with normal and dilated ventricles. *J Magn Reson Imaging* 2008; **28**: 67–73.
30. Anderson JL, Horne BD, Pennell DJ. Atrial dimensions in health and left ventricular disease using cardiovascular magnetic resonance. *J Cardiovasc Magn Reson* 2005; **7**: 671–675.
31. Di Tullio MR, Qian M, Thompson JLP, Labovitz AJ, Mann DL, Sacco RL, Pullicino PM, Freudenberger RS, Teerlink JR, Graham S, Lip GYH, Levin B, Mohr JP, Buchsbaum R, Estol CJ, Lok DJ, Ponikowski P, Anker SD, Homma S, Investigators W. Left atrial volume and cardiovascular outcomes in systolic heart failure: effect of antithrombotic treatment. *ESC Heart Fail* 2018; **5**: 800–808.
32. Lee SL, Daimon M, Nakao T, Singer DE, Shinozaki T, Kawata T, Kimura K, Hirokawa M, Kato TS, Mizuno Y, Watanabe M, Yatomi Y, Yamazaki T, Komuro I. Factors influencing left atrial volume in a population with preserved ejection fraction: left ventricular diastolic dysfunction or clinical factors? *J Cardiol* 2016; **68**: 275–281.